

# A Sampling Measurement of Multimode Waveguide Power\*

E. D. SHARP†, MEMBER, IRE, AND E. M. T. JONES‡, SENIOR MEMBER, IRE

**Summary**—This paper describes a simple method of measuring the total power that is propagating at various frequencies in a multimode, rectangular waveguide. It is particularly useful for determining the power that is generated at harmonic frequencies by high-power transmitters. In this method, the amplitude of the waveguide fields at a number of frequencies is sampled at evenly spaced points around the waveguide periphery. It is shown theoretically that by averaging the squares of the sampled field amplitudes, the total multimode power at the various frequencies can be determined to within  $\pm 2$  or  $\pm 5$  db, depending upon which combinations of waveguide fields are measured. The theoretical accuracy is verified by measurements at both low and high powers.

## I. INTRODUCTION

IN THIS PAPER a simple method is presented for measuring the total power propagating at various frequencies in multimode, rectangular, waveguide. This technique is very useful for quickly and easily determining the multimode harmonic power generated by high-power transmitters.

Basically, the technique described in this paper consists of sampling the waveguide fields at evenly spaced points around the waveguide periphery. Then, from an average of the sampled fields, the total power propagating in rectangular waveguide at a given frequency can be determined to within  $\pm 2$  or  $\pm 5$  db. The fact that this sampling technique does not determine the modal content of the power is not judged to be significant, because it is a demonstrable fact that, due to bends, twists, and other irregularities in any practical waveguide system, the power distribution among the various modes at each frequency is not constant.

There are three principal methods for measuring the harmonic power in a multimode waveguide which may be competitive, in some instances, with the technique described here, although none result in such a compact measuring circuit.<sup>1</sup> One method employs a multitude of directional couplers, each of which couples to a different mode.<sup>2</sup> By measuring the power at the output terminal of each coupler, it is possible in theory to determine the power in each mode at each frequency. How-

ever, in practice it has proved very difficult to construct the appropriate directional couplers, especially in cases where there are more than five modes propagating in the multimode waveguide.

A second method utilizes a large array of probes arrayed along the walls of a waveguide test section.<sup>3-8</sup> By measuring the amplitude and phase of the signals induced in the probes at various frequencies, it has been demonstrated that the power in the various modes at frequencies up to the third harmonic can be readily deduced with the aid of a high-speed digital computer. However, at frequencies above the third harmonic, very poor accuracy is obtained.

The third technique utilizes a series of low-pass dissipative filters placed in series with the transmitter, each of which has a substantial insertion loss.<sup>9</sup> The filters are arranged in the order of their cutoff frequency, with the filter having the highest cutoff frequency nearest the transmitter. By monitoring the power absorbed by each filter, a good measure of the power output of the transmitter in a number of frequency bands is obtained. For example, the filter adjacent to the transmitter measures all the output power of the transmitter above that filter's cutoff frequency. The second filter measures the power incident upon it in the frequency band between its cutoff frequency and that of the preceding filter, etc. In practice, this technique has not proved too satisfactory because of the difficulty in constructing the necessary filters and associated calorimeter equipment.

<sup>3</sup> V. G. Price, "Measurement of harmonic power generated by microwave transmitters," IRE TRANS. ON MICROWAVE THEORY AND TECHNIQUES, vol. MTT-7, pp. 116-120; January, 1959.

<sup>4</sup> V. G. Price, J. P. Rooney and C. Milazzo, "Measurement and Control of Harmonic and Spurious Microwave Energy," General Electric Microwave Lab., Palo Alto, Calif., Final Rept., Phase I, Rept. TIS R 58ELM112, Contract AF 30(602)-1670, No. AD 208290; July 8, 1958.

<sup>5</sup> V. G. Price, R. H. Stone and J. P. Rooney, "Measurement and Control of Harmonic and Spurious Microwave Energy," General Electric Microwave Lab., Palo Alto, Calif., Final Rept., Phase II, Contract AF 30(602)-1670, RADC TR 59-59, No. AD 214430; March 10, 1959.

<sup>6</sup> G. Novick and V. G. Price, "Measurement and Control of Harmonic and Spurious Microwave Energy," General Electric Microwave Lab., Palo Alto, Calif., Final Rept., Phase III, Contract AF 30(602)-1670, RADC TR-172; May 15, 1959.

<sup>7</sup> M. P. Forrer and K. Tomiyasu, "Determination of higher order propagating modes in waveguide systems," *J. Appl. Phys.*, vol. 29, pp. 1040-1045; July, 1958.

<sup>8</sup> C. M. Knop and S. I. Cohn, "A Multiple Probe Method for the Measurement of Reflected and Transmitted Power in a Coaxial Waveguide," *Proc. Nat. Electronics Conf.*, Chicago, Ill., vol. 16, pp. 846-857; 1960.

<sup>9</sup> V. G. Price, "Harmonic calorimeter for power measurements in a multimode waveguide," 1960 IRE INTERNATIONAL CONVENTION RECORD, pt. 3, pp. 136-144.

\* Received by the PGMTT, August 8, 1961; revised manuscript received, October 5, 1961. The work reported in this paper was done at the Stanford Research Institute and was sponsored by the Rome Air Dev. Ctr.; Griffis AFB, N. Y., under Contract AF 30(602)-1998.

† Stanford Research Institute, Menlo Park, Calif.

‡ TRG-West, Palo Alto, Calif.

<sup>1</sup> M. Morelli, "Spurious frequency measurement in waveguide," 1958 IRE NATIONAL CONVENTION RECORD, pt. 8, pp. 176-185.

<sup>2</sup> D. J. Lewis, "Mode couplers and multimode measurement techniques," IRE TRANS. ON MICROWAVE THEORY AND TECHNIQUES, vol. MTT-7, pp. 110-116; January, 1959.

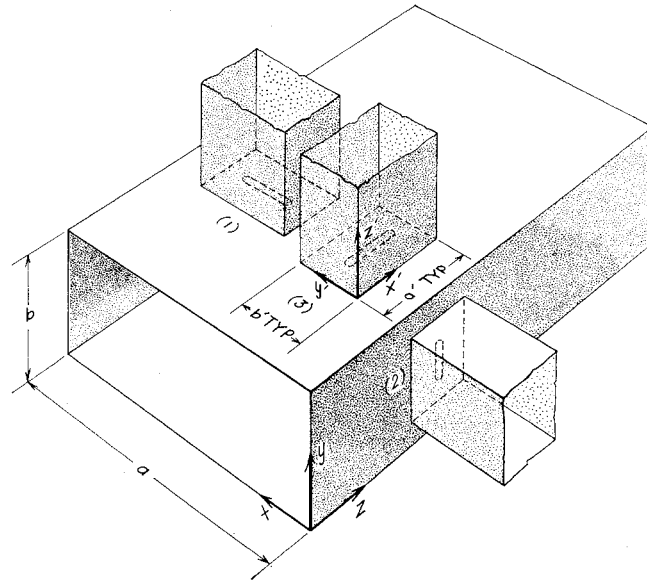


Fig. 1—Typical sampling irises and sampling waveguides mounted on the wall of a rectangular waveguide.

## II. THEORY

### A. General

The sampling method for measuring the multimode power in waveguide utilizes a number of sampling irises or probes placed at evenly spaced points around the periphery of the waveguide.<sup>10</sup> The irises or probes are connected to coaxial lines, or waveguides, containing matched, calibrated, tuned detectors. The detected powers coupled out of the multimode waveguide are averaged, yielding a measurement of the total multimode power at a particular frequency to an accuracy of  $\pm 2$  or  $\pm 5$  db, depending upon which waveguide fields are sampled. The electric field, the magnetic field or both may be sampled. If both the transverse electric and magnetic fields are sampled, the accuracy is about  $\pm 2$  db. If only the transverse electric or transverse magnetic field is sampled, then in most cases, the accuracy is  $\pm 3$  to  $\pm 5$  db.

The measurement of multimode power in rectangular waveguide is discussed in detail; however, the sampling technique described here can also be adapted to measure multimode power in circular waveguide and coaxial transmission line. The theoretical aspects of the measurement of power in multimode waveguide are discussed in this section, and some experimental measurements are given in Section III.

The method used to sample the magnetic field amplitudes is shown in Fig. 1. Long narrow irises are cut in the wall of the multimode waveguide and are connected to smaller sampling waveguides. The irises are long and

narrow, so that they are sensitive to only the component of magnetic field that is parallel to their long dimension. Thus, the irises numbered (1) and (2) sample the transverse magnetic field at the broad and narrow walls, respectively, and the iris numbered (3) samples the longitudinal magnetic field. It can be shown using the small-iris coupling theory of Bethe<sup>11,12</sup> that the power coupled into the sampling waveguide is proportional to the square of the magnetic field incident upon the iris.

The electric field normal to the wall of the multimode waveguide can be sampled by placing small probes at the inside wall of the guide. These probes can be connected to a coaxial transmission line, containing a power detector, to measure the square of the electric field incident upon each probe.

### B. Field Amplitudes in Rectangular Waveguide

Since the field amplitudes at the wall of the multimode waveguide are measured, and not the power, the accuracy of this sampling technique is determined by the variation of field strength between modes relative to the power carried in each mode. Let us write the expressions giving the peak amplitudes of the electric and magnetic fields for the various modes relative to the average power carried in each mode. These expressions can be derived using the expressions for power transfer and waveguide field components given in any standard book covering guided electromagnetic waves.<sup>13</sup> The following equa-

<sup>11</sup> H. A. Bethe, "Lumped Constants for Small Irises," Radiation Lab., Mass. Inst. Tech., Cambridge, Report 43-22, p. 27; March, 1943.

<sup>12</sup> A. T. Starr, "Radio and Radar Techniques," Pitman Publishing Corp., New York, N. Y.; 1953.

<sup>13</sup> S. Ramo and J. R. Whinnery, "Fields and Waves in Modern Radio," John Wiley and Sons, Inc., New York, N. Y., 2nd ed., pp. 349-353, 366; 1953.

<sup>10</sup> E. D. Sharp and E. M. T. Jones, "A Sampling Technique for the Measurement of Harmonic Power in Multimode Waveguide," Stanford Res. Inst., Menlo Park, Calif., Tech. Note 3, Contract AF 30(602)-1998; February, 1961.

tions apply for the field components in the rectangular waveguide of Fig. 1:

$$\begin{aligned}
 |H_x|_{\text{TE}_{mn}}^2 &= K \frac{\frac{m^2\pi^2}{a^2} \sqrt{1-f_c^2/f^2}}{k_c^2(1+\delta_{n0})} P_{\text{TE}_{mn}} = \frac{(1-f_c^2/f^2)}{\eta^2} |E_y|_{\text{TE}_{mn}}^2 \\
 |H_x|_{\text{TM}_{mn}}^2 &= K \frac{\frac{n^2\pi^2}{b^2}}{k_c^2\sqrt{1-f_c^2/f^2}} P_{\text{TM}_{mn}} = \frac{|E_y|_{\text{TM}_{mn}}^2}{\eta^2(1-f_c^2/f^2)} \\
 |H_y|_{\text{TE}_{mn}}^2 &= K \frac{\frac{n^2\pi^2}{b^2} \sqrt{1-f_c^2/f^2}}{k_c^2(1+\delta_{m0})} P_{\text{TE}_{mn}} = \frac{(1-f_c^2/f^2)}{\eta^2} |E_x|_{\text{TE}_{mn}}^2 \\
 |H_y|_{\text{TM}_{mn}}^2 &= K \frac{\frac{m^2\pi^2}{a^2}}{k_c^2\sqrt{1-f_c^2/f^2}} P_{\text{TM}_{mn}} = \frac{|E_x|_{\text{TM}_{mn}}^2}{\eta^2(1-f_c^2/f^2)} \\
 |H_z|_{\text{TE}_{mn}}^2 &= K \frac{1}{f^2/f_c^2\sqrt{1-f_c^2/f^2}(1+\delta_{m0})(1+\delta_{n0})} P_{\text{TE}_{mn}} \\
 k_c^2 &= m^2\pi^2/a^2 + n^2\pi^2/b^2 \quad \delta_{n0} = 1, \quad \text{if } n = 0 \\
 \delta_{n0} &= 0, \quad \text{if } n \neq 0 \quad K = 8/ab\eta
 \end{aligned} \tag{1}$$

where  $f_c$  is the cutoff frequency of each mode considered,  $f$  is the frequency,  $\eta$  is the free-space impedance  $120\pi$ , and  $P$  is the average power carried by each mode. All of the peak  $E$ - and  $H$ -fields in (1) occur at one or the other (or both) of the broad and narrow waveguide walls.

To achieve good accuracy, four different sets of field quantities may be sampled. These four are listed below:

- 1) Both the transverse electric and transverse magnetic fields at both the broad and narrow walls.
- 2) The broad- and narrow-wall transverse magnetic fields and the longitudinal magnetic field.
- 3) The broad- and narrow-wall transverse magnetic fields.
- 4) The broad- and narrow-wall transverse electric fields.

Since the power in a multimode waveguide is determined by adding the squares of the various sampled fields, the accuracy of the sampling technique can be determined by adding the squares of the fields in each set listed above. Adding the squares of both the transverse electric and transverse magnetic fields of each mode at both the broad and narrow walls, we find that (omitting

modal subscript notation)

$$\begin{aligned}
 |H_x|^2 + |H_y|^2 + \left| \frac{E_x}{\eta} \right|^2 + \left| \frac{E_y}{\eta} \right|^2 \\
 = \frac{(2-f_c^2/f^2)KP}{(1+\delta_{n0})(1+\delta_{m0})\sqrt{1-f_c^2/f^2}} \tag{2}
 \end{aligned}$$

for both TE and TM modes. We see from (2) that the variation in the sum of the squares of the peak field intensities depends upon the ratio of the cutoff frequency of a particular mode to the operating frequency, and upon whether or not the mode has a uniform variation in field across one waveguide wall.

The sum of the peak field intensities is plotted in Fig. 2, assuming  $KP=1$ . From Fig. 2 we see that the variation in the sum of the squares of the field intensities is less than  $\pm\frac{1}{2}$  db for  $f_c/f \leq 0.86$ , for either those modes having  $m \neq 0$  and  $n \neq 0$ , or those modes having  $m=0$  or  $n=0$ . However, there is a constant 3-db difference between these two types of modes, so that accuracy of measurement is  $\pm 2$  db for  $f_c/f \leq 0.86$ . In Fig. 3 we see a typical situation in which there are several waveguide modes propagating; here the operating frequency is 8.25 Gc, which is the third harmonic frequency of 2.75 Gc, a frequency in the operating band of  $2.84 \times 1.34$ -in waveguide. At 8.25 Gc, the total variation in the sum of the peak field intensities is less than  $\pm 2.5$  db. Thus, by

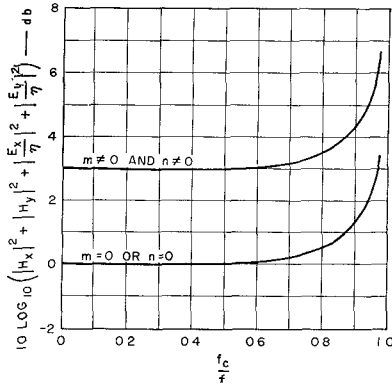


Fig. 2—Sum of the squares of the broad- and narrow-wall peak-transverse electric and peak-transverse magnetic fields for modes propagating in rectangular waveguide.

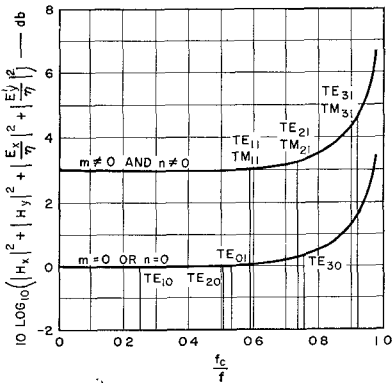


Fig. 3—Sum of the squares of the broad- and narrow-wall peak-transverse electric and peak-transverse magnetic fields in rectangular waveguide for modes propagating at the third harmonic.

measuring the sum of the peak field intensities, the total power propagating in the multimode waveguide can be determined to within  $\pm 2.5$  db. As the frequency is raised, the position of the modes moves to the left, and new propagating modes appear at the right. At any frequency the field variation between modes is about the same, but at the higher frequencies more modes are grouped near  $f_c/f = 1$ .

The accuracy obtainable by sampling the second set of field quantities listed above is now determined. Adding the squares of all the magnetic field components for each mode, we find that (omitting modal subscript notation)

$$|H_x|^2 + |H_y|^2 + |H_z|^2 = \frac{KP}{(1 + \delta_{m0})(1 + \delta_{n0})\sqrt{1 - f_c^2/f^2}} \quad (3)$$

for both TE and TM modes. In this case also, the variation in the sum of the squares of the peak field intensities depends upon  $f_c/f$ , and upon whether or not the mode has field variations across one or both waveguide walls. The field intensities of (3) are plotted in Fig. 4, assuming that  $KP = 2$  (so that the curves of Figs. 2 and 4 are normalized alike). In Fig. 4 the total variation in

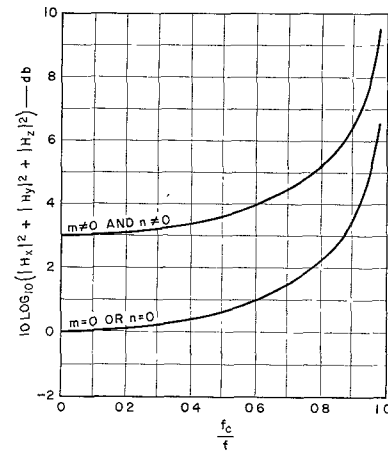


Fig. 4—Sum of the squares of all the peak-components of magnetic field for modes propagating in rectangular waveguide.

the sum of the field strengths is  $\pm 3$  db for  $f_c/f \leq 0.86$ , as compared to the  $\pm 2$  db shown in Fig. 2. If we imagine that the modes of Fig. 3 at the third harmonic frequency are superimposed upon Fig. 4, the total variation in the field strengths would be  $\pm 3.5$  db. The total power at the third harmonic could thus be measured to within  $\pm 3.5$  db by sampling all possible components of magnetic field.

The accuracies obtainable by sampling the third and fourth sets of field quantities listed, are determined by summing the squares of the appropriate field quantities as follows (omitting modal subscript notation):

$$\begin{aligned} |H_x|^2 + |H_y|^2 &= \frac{KP\sqrt{1 - f_c^2/f^2}}{(1 + \delta_{m0})(1 + \delta_{n0})} \\ &= (1 - f_c^2/f^2) \left( \left| \frac{E_x}{\eta} \right|^2 + \left| \frac{E_y}{\eta} \right|^2 \right) \quad (4) \end{aligned}$$

for TE modes.

$$\begin{aligned} |H_x|^2 + |H_y|^2 &= \frac{KP}{\sqrt{1 - f_c^2/f^2}} = \left( \left| \frac{E_x}{\eta} \right|^2 + \left| \frac{E_y}{\eta} \right|^2 \right) / (1 - f_c^2/f^2) \quad (5) \end{aligned}$$

for TM modes. The field intensities of (4) and (5) are plotted in Figs. 5 and 6, assuming that  $KP = 2$ . It is seen that the variation of the fields in both cases is about the same. If the third harmonic frequency modes of Fig. 3 are superimposed upon Figs. 5 and 6, we find that the total variation in the transverse magnetic fields is about  $\pm 4.4$  db, and that the total variation in transverse electric fields is about  $\pm 4$  db.

The accuracy obtainable by measuring combinations of various field quantities has been discussed above. In general, the accuracy is best when most of the available fields are measured. In the interest of developing the simplest technique, it is desirable to measure the least number of field quantities. The measurement of either the transverse magnetic field or transverse electric field is the simplest method of those listed. In a high-power

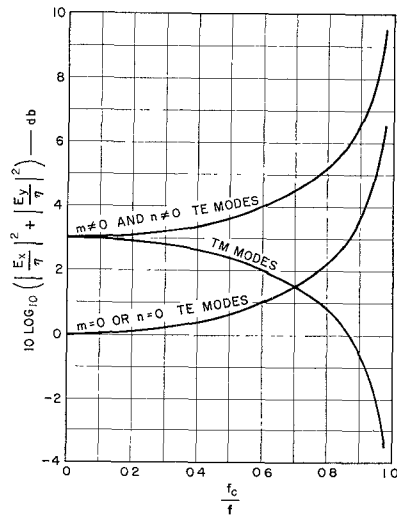


Fig. 5—Sum of the squares of the broad- and narrow-wall peak-transverse electric fields for modes propagating in rectangular waveguide.

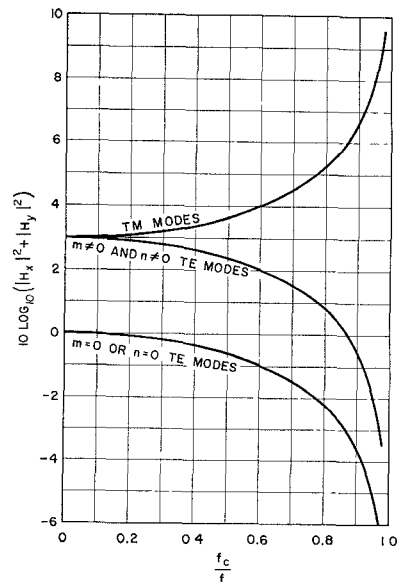


Fig. 6—Sum of the squares of the broad- and narrow-wall peak-transverse magnetic fields for modes propagating in rectangular waveguide.

system it is preferable to place irises rather than probes in the wall of a waveguide because irises are much less susceptible to power breakdown. Thus the simplest and most practical method of measuring multimode power in high-power waveguide is that of measuring the transverse magnetic field.

In Figs. 7-9 the variation of the transverse magnetic field strengths is shown for the second through fifth harmonic frequencies of 2.75 Gc, a frequency in the operating band of  $2.84 \times 1.34$ -in waveguide. At all four harmonic frequencies, most of the modal variations in magnetic field strengths are within  $\pm 5$  db, and the accuracy of the sampling device measuring the transverse magnetic field is expected to be  $\pm 5$  db. This accuracy should hold at even higher harmonic frequencies.

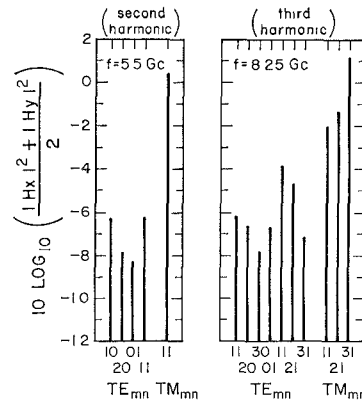


Fig. 7—Mean square of broad-wall and narrow-wall relative-peak-transverse H-fields for each propagating mode in S-band waveguide—second harmonic and third harmonic.

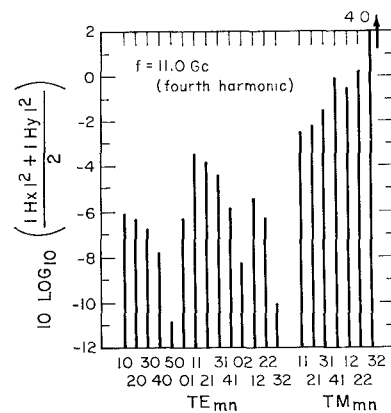


Fig. 8—Mean square of broad-wall and narrow-wall relative-peak-transverse H-fields for each propagating mode in S-band waveguide—fourth harmonic.

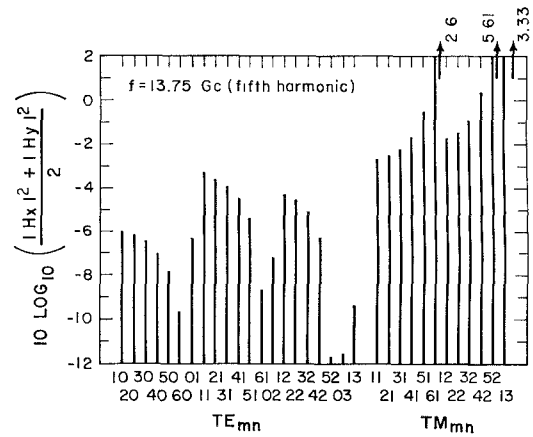


Fig. 9—Mean square of broad-wall and narrow-wall relative-peak-transverse H-fields for each propagating mode in S-band waveguide—fifth harmonic.

### C. Theory of Multimode Sampling Technique in Rectangular Waveguide

In the described measuring scheme the  $H$ -field is determined by measuring the power coupled through an iris into a sampling waveguide. The following discussion can also be applied to the measurement of  $E$ -field using a probe connected to a coaxial line. The power coupled through a single iris cut in the wall of the multimode waveguide is proportional to the square of the resultant  $H$ -field in the multimode waveguide at the iris. This resultant  $H$ -field is the phasor sum of the  $H$ -fields of all the propagating modes. The sampled power at a particular iris may be strong or weak, depending upon the resultant  $H$ -field at the iris. However, by placing several evenly spaced irises across the broad and narrow walls of the waveguide, and by averaging the coupled powers, it can be shown that for modes with a different number of variations along one waveguide wall, the sum of the squares of the peak  $H$ -field strengths is measured. That is, the total multimode power is sampled independently of the relative phases between modes.

In order to demonstrate that modes with a different number of field variations are sampled independently, consider the transverse  $H$ -field at the broad wall of the multimode waveguide which can be written as follows:

$$H\left(\frac{x}{a}\right) = \sum_{m=0}^M H_m \sin \frac{m\pi x}{a} \quad (6)$$

where  $H_m$  is the phasor sum of the peak  $H$ -fields of modes with  $m$  variations across the wall. If the square of the magnitude of the  $H$ -field, which is found by multiplying (6) by its complex conjugate, is integrated across the broad wall, we find that the fields with different variations contribute to the integral independently

$$\int_0^1 \left| H\left(\frac{x}{a}\right) \right|^2 d\left(\frac{x}{a}\right) = \frac{1}{2} \sum_{m=1}^M |H_m|^2. \quad (7)$$

Referring to (12), derived in the Appendix, we find that the above integral is also equal to the average of the squares of the  $H$ -fields sampled at each sampling iris. Substituting (12) into (7) we find that

$$\frac{1}{M'} \sum_{n=1}^{M'} \left| H\left(\frac{n}{M'}\right) \right|^2 = \frac{1}{2} \sum_{m=1}^M |H_m|^2 (M' > M). \quad (8)$$

Since the power sampled at each iris is proportional to the square of the incident  $H$ -field, the term on the left of (8) is proportional to the average of the powers sampled through  $M'$  evenly spaced irises. Thus from (8) we can conclude that by averaging the powers sampled at the broad wall, modes with different numbers of variations across the broad wall are sampled independently. Modes with the same number of variations across the broad wall are sampled in proportion to the square of

the phasor sum of their  $H$ -fields. For evenly spaced irises across the narrow wall the situation is analogous.

Conveniently, most modes which are not sampled independently at one wall are sampled independently at the other wall. The errors, arising when modes having the same number of variations along a wall are sampled, can be minimized by placing two or more rows of irises in the waveguide wall and averaging the total multimode power measured at each row. If the waveguide system is badly mismatched at the harmonic frequency, high standing waves occur also making it desirable to use more than one row of sampling irises.

### D. Procedure for Reducing Data in Rectangular Waveguide

The experimental procedure to use indicated by the above results is as follows: irises sensitive to the transverse  $H$ -field are cut at evenly spaced points across broad and narrow walls of the waveguide. The number of irises in each wall is equal to the number of field variations at the wall of the highest-order propagating mode. Actually, according to (8), there should be at least one more iris than the number of field variations, but there is no need for one extra iris because it would be placed at the corner of the waveguide where the transverse  $H$ -field is zero. To determine the total power in the multimode waveguide, average the sampled powers at the broad wall by dividing the sum of the sampled powers by one plus the number of broad-wall irises. Next, average the sampled powers at the narrow wall by dividing the sum of the sampled powers by one plus the number of narrow-wall irises. Then, average the narrow- and broad-wall average sampled powers to get a resultant average. To find the total power in the multimode waveguide, divide the resultant average by the calibration of the irises.

The calibration is set equal to the average power coupling between the  $TE_{10}$  mode in the multimode waveguide and the mode in the broad-wall sampling waveguides; the  $TE_{10}$  mode power coupling is approximately the mean coupling of all the propagating modes in the multimode waveguide. The approximate theoretical power coupling between the  $TE_{10}$  mode in the multimode waveguide and the mode in the broad-wall sampling waveguides is derived, using Bethe's small-iris coupling theory, to be

$$C_{TE_{10}} = \frac{16\pi^2 M^2 \sqrt{1 - f_c^2/f^2}}{aba'b'\lambda\lambda_g'} \sin^2 \frac{\pi x}{a} \quad (9)$$

where  $M$  is the magnetic polarizability parallel to the long dimension of the iris,  $x$  is the position of the iris in the broad wall of the multimode waveguide,  $\lambda$  is the free-space wavelength, and  $\lambda_g'$  is the guide wavelength in the sampling waveguide. The other quantities are defined in Fig. 1 and (1). The magnetic polarizability,

$M$ , of long, narrow irises has been measured by Cohn.<sup>14</sup> The irises can be calibrated experimentally by exciting a pure  $TE_{10}$  mode in the multimode waveguide by using a long taper between a single-mode waveguide and the multimode waveguide, and then measuring the coupling between the multimode and broad-wall sampling waveguides.

The averaging processes used to find the total multimode power can be carried out by using an appropriate adding circuit connected to the outputs of the detectors in the sampling waveguides. An example of such a circuit is shown in Fig. 10. By its use, a continuous and instantaneous measurement of the power, propagating at each harmonic frequency, is possible.

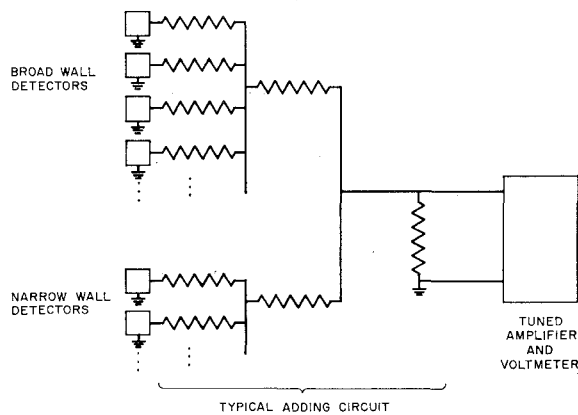


Fig. 10—Typical adding circuit.

### III. EXPERIMENTAL MEASUREMENTS

#### A. Low-Power Measurements

To verify the theoretical analysis presented in the previous section, low-power measurements were made using an experimental model of the multimode power sampler. Different modal distributions of known total power were excited in the multimode waveguide, and in each case a measurement of the total power was made to check the accuracy of the power sampler. The measurements were made at the fifth harmonic frequency. Since 33 modes can propagate at the fifth harmonic, measurements at this frequency should provide a severe test of the performance of the multimode power sampler.

A photograph of the experimental model is shown in Fig. 11. It has six sampling irises cut in the broad wall and two in the narrow wall of an  $S$ -band ( $2.84 \times 1.34$ -in ID) waveguide. The irises are evenly spaced across their respective walls in two closely spaced rows 0.350 in apart. Two rows are used because the dimensions of the irises ( $0.350 \times 0.094$  in) prevent the use of one row. The two rows are spaced closely enough so that the differen-

tial phase shift between rows for modes that are far from cutoff is quite small (*i.e.*, about  $10^\circ$ ). The differential phase shift between rows comparing a mode close to cutoff and one that is far from cutoff, however, is much greater (*i.e.*, over  $60^\circ$ ). A  $K_u$ -band ( $0.622 \times 0.311$  in ID) sampling waveguide containing a calibrated matched tuned detector is placed in turn over each iris to measure the power sampled at each iris. An area the size of the detecting waveguide is cut into the  $S$ -band waveguide wall around each iris to provide for accurate positioning of the detecting waveguide. Adequate electrical contact between the detecting waveguide and  $S$ -band waveguide is obtained by applying moderate pressure by hand. All irises, except the one under measurement, were short-circuited to prevent them from radiating, by placing aluminum tape over them. The calibration defined in Section II-D was measured to be  $2.63 \times 10^{-3}$ .

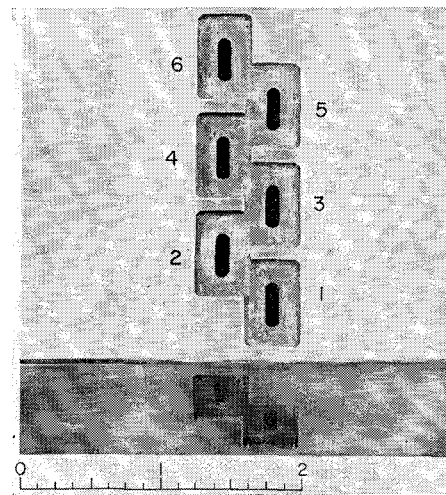


Fig. 11—Sampling irises cut in the wall of an  $S$ -band waveguide.

To provide a good experimental verification of the theory, many higher modes should be excited in the  $S$ -band waveguide and the power distribution among the modes should be variable. To do this, power was fed from an input waveguide through a resonant iris directly into the  $S$ -band waveguide as indicated in Fig. 12. The input waveguide was soldered to a flat plate containing the resonant iris, and the flat plate was clamped to the  $S$ -band waveguide flange in several positions to excite different modal distributions of power. The total power coupled through the resonant iris into the  $S$ -band waveguide was determined experimentally as the difference between the incident and reflected power in the input waveguide. To determine the accuracy of this measuring scheme, the power measured by the power sampler was compared to the known power entering the  $S$ -band waveguide. The appropriate modal distribution of power was theoretically determined by matching an assumed field in the iris to the modal fields in the multimode waveguide.

<sup>14</sup> S. B. Cohn, "Determination of aperture parameters by electrolytic-tank measurements," Proc. IRE, vol. 39, pp. 1416-1421; November, 1951.

Several experimental results are now given. Measurements were first made at a frequency of 13.6 Gc with a load made up of tapered resistance cards inserted at the end of the *S*-band waveguide. This load seemed to adequately terminate all the excited modes, because movement of the load changed the sampled power readings by less than 0.2 db. Several measurements for different mode excitations and for several lengths of *S*-band waveguide inserted between the input and irises are listed in Table I.

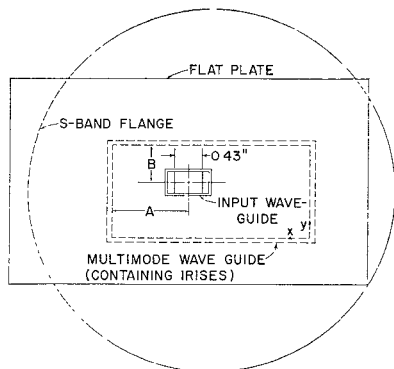


Fig. 12—Multimode exciter.

TABLE I  
POWER MEASURED RELATIVE TO KNOWN POWER (db)  
( $f=13.6$  Gc) (WAVEGUIDE TERMINATED)

Position of Input Waveguide with Respect to <i>S</i> -Band Waveguide Cross Section ( <i>A</i> and <i>B</i> in in.)	Power (db) for Various Distances between Input Waveguide and Row of Irises (in.)			
	14	20	22	24
Centered ( $A=1.42, B=0.67$ )	-1.6	0.1	-1.8	-0.6
Off-Center (1) ( $A=0.82, B=0.50$ )	3.73	5.5	5.5	1.7
Off-Center ( $A=1.22, B=0.50$ ) and Rotated $90^\circ$	-3.6	0.5	3.6	3.4

Other measurements which were made at a frequency at 13.75 Gc with the *S*-band waveguide open-ended and radiating into absorbing material, are listed in Table II. The frequency of 13.75 Gc was chosen because it is only one per cent above the cutoff frequency of the  $TE_{52}$  and  $TM_{52}$  modes, making the termination of these modes very difficult. The modes close to cutoff are strongly reflected at a small horn or open-ended waveguide, while lower-order modes are not. The measurements given in Table II indicate the accuracy to be expected if the power were measured just prior to its entering a small horn antenna.

In Table I the largest deviation in power measurement is  $-3.6$  and  $5.5$  db, which is almost within  $\pm 5$  db of the correct power. Comparing Tables I and II for the case where the input waveguide is centered, it is seen that at 13.75 Gc the measured power is 6–8 db too high and at 13.6 Gc the measured power is about 1 db too

TABLE II  
POWER MEASURED RELATIVE TO KNOWN POWER (db)  
( $f=13.75$  Gc) (OPEN-ENDED WAVEGUIDE)

Position of Input Waveguide with Respect to <i>S</i> -Band Waveguide Cross Section ( <i>A</i> and <i>B</i> in in.)	Power (db) for Various Distances between Input Waveguide and Row of Irises (in.)			
	14	20	22	24
Centered ( $A=1.42, B=0.67$ )	6.1	7.9	7.5	3.1
Off-Center (1) ( $A=0.82, B=0.50$ )	4.3	5.5	6.5	5.1
Off-Center (2) ( $A=1.22, B=0.33$ )	1.4	0.4	3.6	3.3
Off-Center (3) ( $A=0.82, B=0.84$ )	6.2	1.6	2.8	4.7

low. The main reason for this difference is that the  $TM_{52}$  mode is strongly excited when the input waveguide is centered. It does not propagate at 13.6 Gc but does propagate at 13.75 Gc, having very strong *H*-fields at both the broad and narrow walls. With the input waveguide at the second off-center position of Table II, the  $TM_{52}$  mode is not excited, and accordingly, the readings are better estimates of the actual power. Another factor helping to make the error large is that the  $TM_{52}$  mode is strongly reflected at the open end of the waveguide setting up a standing wave in this mode. The only modes excited when the input waveguide is centered are modes with an odd number of variations in the *x*-dimensions and an even number of variations in the *y*-dimension; of these excited modes the  $TM_{52}$  is the only one with abnormally strong *H*-fields at both broad and narrow walls.

Comparing Tables I and II for the input waveguide at the off-center position (1), the measured powers are about the same at 13.6 and 13.75 Gc in contrast to the measured powers for the input waveguide centered. The reason for this behavior with the input waveguide at the off-center position (1) is probably due to the excitation of modes such as the  $TM_{13}$  which propagate at both 13.6 and 13.75 and have strong *H*-fields. Note that the  $TM_{13}$  mode is not excited when the input waveguide is centered. Most of the other power readings in Tables I and II are within 5–6 db of the correct power.

The measurements were made at several cross sections along the waveguide to determine the effect of the phase difference between modes. As explained in the previous section, the modes with a different number of variations across the waveguide wall are sampled independently of their relative phases. On the other hand, the sampling of modes with the same number of variations across the wall is dependent upon their relative phases. The above measurements indicate that even though some modes have the same number of *H*-field variations the accuracy of this measuring scheme is not seriously affected.

Another set of measurements was made at 13.75 Gc with two  $90^\circ$  bends—an *E*-plane and an *H*-plane bend—inserted in series between the iris section and the open-



ended waveguide. The accuracy obtained here was very similar to that shown in Table II, and it can be concluded that reflections from waveguide bends have little effect upon the accuracy of this measuring scheme.

### B. High-Power Measurements

Since the low-power measurements were quite successful in demonstrating the operation of the multimode power sampler, a second experimental model was designed to measure the harmonic powers generated by a high-power transmitter. The experimental model designed to measure the second through fifth harmonic frequencies generated by a QK-338 high-power S-band magnetron is shown in Fig. 13. The set of waveguides on the right samples the third harmonic, the center set samples the fourth and fifth harmonic, and the set on the left samples the second harmonic. Irises similar to those shown in Fig. 11 connect the multimode waveguide to the sampling waveguides.

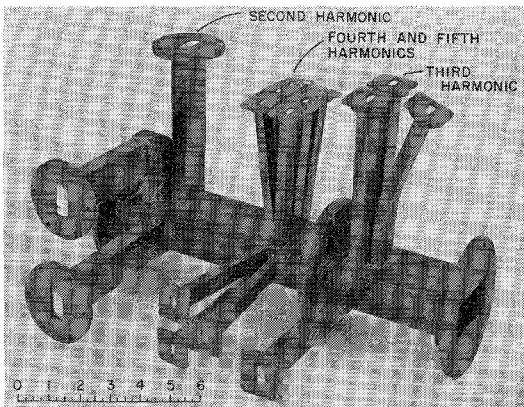


Fig. 13—Multimode power sampler of second through fifth harmonic frequencies.

The harmonic frequency powers measured using the experimental model are shown in Table III.<sup>15</sup> As a comparison the General Electric Microwave Laboratory, using the array of probes mounted in the waveguide wall, measured the total third harmonic power to be 4 db above the 2190-w peak shown in Table III. The agreement between the two measurements is adequate, considering that the high-power load used in the measurement undoubtedly provided a poor match to the higher-order propagating modes, and that the accuracy of the probe array depends upon all the propagating modes being terminated in a matched load.<sup>3-7</sup>

The detecting circuit used to measure the sampled power is shown in Fig. 14. The size of the sampling waveguide, which acts as a high-pass filter, and the cutoff frequency of the low-pass filter are chosen so that only the correct harmonic frequency enters the detector.

<sup>15</sup> The General Electric Microwave Lab. kindly offered the use of their high-power facilities for this measurement.

TABLE III  
PEAK POWERS GENERATED BY QK-338 MAGNETRON

Frequency	Peak Power (w)
Fundamental (2791 Mc)	$4.2 \times 10^6$
Second harmonic	330
Third harmonic (8379 Mc)	2190
Fourth harmonic	52
Fifth harmonic	7

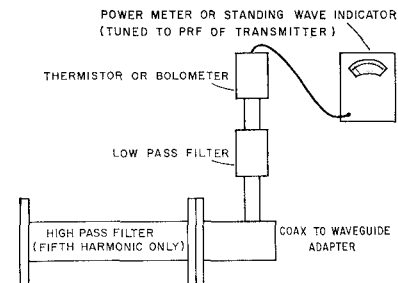


Fig. 14—Sampled-power-detecting circuit.

## IV. CONCLUSIONS

A simple technique using compact instrumentation for the measurement of power at various frequencies in multimode rectangular waveguide has been demonstrated both theoretically and experimentally. The accuracy of  $\pm 2$  or  $\pm 5$  db should be adequate for most purposes. It is expected that this method will be useful in the measurement of harmonic powers generated by high-power transmitters.

## APPENDIX

### THE SAMPLING OF MULTIMODE POWER IN A WAVEGUIDE

The sampling of a signal, at regular time intervals, is analogous to the sampling of the fields of a multimode waveguide at regularly spaced points across the wall of the waveguide. Here, a result of the theory of sampled signals which are functions of time is applied by analogy to the sampling of fields in a waveguide. It can be shown that<sup>10,16</sup> for a signal which is a function of time the following relationship holds:

$$\int_0^T [G(t)]^2 dt = \frac{1}{2W} \sum_{n=1}^{2TW} \left[ G\left(\frac{n}{2W}\right) \right]^2 \quad (10)$$

where  $G(t)$  is a signal that is made up of a finite number of Fourier components in the frequency band  $0 \leq f < W$ . The integral on the left of (10) is the integral of the square of the signal over one period, and the summation on the right of (10) is the sum of the sample values of the square of the signal taken at evenly spaced sample points.

<sup>16</sup> S. Goldman, "Information Theory," Prentice-Hall, Inc., Englewood Cliffs, N. J., pp. 80-83; 1953.

The analogy between signals in the time domain and the fields in the transverse plane of a waveguide is now made. For a specific example take the transverse  $H$ -field near the broad wall of a multimode waveguide. The transverse  $H$ -field near the broad wall of the multimode waveguide contains field components of the form

$$H\left(\frac{x}{a}\right) = \sum_{m=1}^M H_m \sin m\pi \frac{x}{a} \quad (11)$$

where  $M$  is the maximum number of  $H$ -field variations across the broad wall of the waveguide. If the normalized distance  $(x/a)$  across the waveguide is made analogous to time  $(t)$ , the transverse  $H$ -field of (11) becomes analogous to the signal  $G(t)$  of (10); also, the quantity  $[m\pi(x/a)]$  becomes analogous to the product of angular frequency and time  $(\omega t)$ , or the index  $(m)$  becomes analogous to twice the signal frequency  $(2f)$ . Note that the time interval  $0 < t < T$  corresponds to the length interval  $0 < x/a < 1$ , and that the frequency band of the signal  $0 < 2f < 2W$  corresponds to the number of variations of  $H$ -field being limited between  $0 < M < M'$ , where

$M'$  is an integer greater than  $M$ . Note that the analogy between  $H(x/a)$  and  $G(t)$  is not quite exact, because  $H(x/a)$  can be complex and  $G(t)$  is real; however, (12) analogous to (10) can be derived in the following way:

- 1) Make the real part of  $H(x/a)$  analogous to  $G(t)$  and apply the other analogies given above to (10).
- 2) Make the imaginary part of  $H(x/a)$  analogous to  $G(t)$  and apply the other analogies given above to (10).
- 3) Add the results of 1) and 2), noting that the magnitude squared of a complex variable is equal to the sum of the squares of the real and imaginary parts.

Thus

$$\int_0^1 \left| H\left(\frac{x}{a}\right) \right|^2 d\left(\frac{x}{a}\right) = \frac{1}{M'} \sum_{n=1}^{M'} \left| H\left(\frac{n}{M'}\right) \right|^2. \quad (12)$$

Results similar to (12) are obtained if the field across the narrow wall of a rectangular waveguide or around the circumference of a circular waveguide is considered.